MNRAS 000, 1–7 (2018) Preprint 13 April 2018 Compiled using MNRAS LATEX style file v3.0

Falsifying ΛCDM: Model-independent tests of the concordance model with eBOSS DR14Q and Pantheon

Arman Shafieloo,[1,2]★ Benjamin L'Huillier,[1] and Alexei A. Starobinsky[3,4]
[1] Korea Astronomy and Space Science Institute, Yuseong-gu, Daedeok-daero 776, Daejeon 34055, Korea
[2] University of Science and Technology, Yuseong-gu 217 Gajeong-ro, Daejeon 34113, Korea
[3] L. D. Landau Institute for Theoretical Physics RAS, Moscow 119334, Russia
[4] National Research University Higher School of Economics, Moscow 101000, Russia

Accepted XXX. Received YYY; in original form ZZZ

ABSTRACT

We combine model-independent reconstructions of the expansion history from the latest Pantheon supernovae distance modulus compilation and measurements from baryon acoustic oscillation to test some important aspects of the concordance model of cosmology namely the FLRW metric and flatness of spatial curvature. We then use the reconstructed expansion histories to fit growth measurement from redshift-space distortion and obtain strong constraints on $(\Omega_m, \gamma, \sigma_8)$ in a model independent manner. Our results show consistency with a spatially flat FLRW Universe with general relativity to govern the perturbation in the structure formation and the cosmological constant as dark energy. However, we can also see some hints of tension among different observations within the context of the concordance model related to high redshift observations ($z > 1$) of the expansion history. This supports earlier findings of Sahni et al. (2014) & Zhao et al. (2017) and highlights the importance of precise measurement of expansion history and growth of structure at high redshifts.

Key words: methods: numerical – methods: statistical – large-scale structure of Universe – cosmology: theory – cosmological parameters – dark energy –

1 INTRODUCTION

The concordance model of cosmology is based on Einstein's general theory of relativity (GR), which enabled us to come up with a theory of the Universe that is testable and can be falsified. The concordance flat ΛCDM model, which is based on GR and the assumptions of isotropy and homogeneity of the Universe, has been very successful at explaining various astronomical observations. This predictive model explains the dynamics of the Universe with only 6 free parameters. Ω_b and Ω_{dm} (baryonic and dark matter densities) are the matter parameters. Assuming a flat universe and cosmological constant being responsible for late time acceleration of the Universe, we can derive $\Omega_\Lambda = 1 - (\Omega_b + \Omega_{dm})$. τ representing the epoch of reionization, H_0 the Hubble parameter, n_s the spectral index of the primordial spectrum and A_s the overall amplitude of the primordial spectrum are the other 4 parameters of this model. Out of these parameters, the first four dictate the dynamic of the Universe and the other two represent the initial condition through the primordial fluctuations given by $P_R(k) = A_s \left(\frac{k}{k_*}\right)^{n_s - 1}$, where k_* is the pivot point. Having the form of the primordial fluctuations and the expansion history of the Universe one can determine the growth of structure for this model on linear scales following the linearised perturbation equation and also run N-body simulations to study the small scales and non-linear regime. Despite the simplicity of the model, most astronomical observations are in great agreement with the concordance model and so far there has not been any strong observational evidence against it (e.g., Planck Collaboration XIII 2016; Alam et al. 2017; Scolnic et al. 2017). In this paper we test some important aspects of the concordance model of cosmology in light of the most recent cosmological observations in a model-independent manner. We test dark energy as the cosmological constant Λ, the FLRW metric and the flatness of the Universe, and we derive the $H_0 r_d$ parameter. We then use model independent reconstruction of the expansion history from supernovae data to fit growth of structure data and put model independent constrains on key cosmological parameters of $(\Omega_m, \gamma$ and $\sigma_8)$. In § 2 we describe the background expansion and our tests on Λ dark energy, FLRW metric and flatness of the spatial curvature. Analysis on the growth of structure and testing general theory of relativity are presented in § 3, and our conclusions are drawn in § 4.

★ E-mail: shafieloo@kasi.re.kr (AS), benjamin@kasi.re.kr (BL), alstar@landau.ac.ru (AAS)

2 BACKGROUND EXPANSION: TESTING Λ THE FLRW METRIC, AND THE CURVATURE

At the background level, it is possible to test dark energy as Λ, the FLRW metric, and the curvature of the Universe. In a FLRW universe with a dark energy component of equation of state $w(z)$, the luminosity distance can be written for any curvature Ω_k

$$d_{\rm L}(z) = \frac{c}{H_0}(1+z)\mathcal{D}(z), \tag{1}$$

where

$$\mathcal{D}(z) = \frac{1}{\sqrt{-\Omega_k}}\sin\left(\sqrt{-\Omega_k}\int_0^z \frac{{\rm d}x}{h(x)}\right) \tag{2}$$

is the dimensionless comoving distance, and

$$h^2(z) = \left(\frac{H(z)}{H_0}\right)^2 = \Omega_{\rm m}(1+z)^3 + \Omega_k(1+z)^2 + (1-\Omega_{\rm m}-\Omega_k)\exp\left(3\int_0^z \frac{1+w(x)}{1+x}{\rm d}x\right) \tag{3}$$

is the expansion history. Having different observables of the cosmic distances and expansion history one can then introduce novel approaches to examine the FLRW metric, flatness of the Universe and Λ dark energy in a model-dependent (e.g., Farooq & Ratra 2013) or independent way (Clarkson et al. 2008; Sahni et al. 2008; Sapone et al. 2014; L'Huillier & Shafieloo 2017; Zhao et al. 2017; Marra & Sapone 2017). Note that one can also test the metric and the curvature using gravitational lensing (e.g. Räsänen et al. 2015; Denissenya et al. 2018).

2.1 Model-independent reconstruction of the expansion history from the Pantheon compilation

In order to reconstruct the expansion history $h(z)$ at any redshift z, we apply the iterative smoothing method (Shafieloo et al. 2006; Shafieloo 2007; L'Huillier & Shafieloo 2017) to the the latest compilation of supernovae distance modulus (Pantheon, Scolnic et al. 2017). In order to take into account the non-diagonal terms of the covariance matrix, we modified the method in the following way. Starting with some initial guess $\hat{\mu}_0$, we iteratively calculate the reconstructed $\hat{\mu}_n + 1$ at iteration $n+1$:

$$\hat{\mu}_{n+1}(z) = \hat{\mu}_n(z) + N(z)\,\boldsymbol{\delta\mu}_n^{\rm T}\cdot\mathbf{C}_{\rm SN}^{-1}\cdot\boldsymbol{W}(z), \tag{4}$$

where

$$\boldsymbol{W}_i(z) = \exp\left(-\frac{\ln^2\left(\frac{1+z}{1+z_i}\right)}{2\Delta^2}\right) \tag{5}$$

is a vector of weights,

$$N^{-1}(z) = \mathbb{1}^T\cdot\mathbf{C}_{\rm SN}^{-1}\cdot\boldsymbol{W}(z) \tag{6}$$

is a normalization factor

$$\mathbb{1} = (1,\ldots,1)^T \tag{7}$$

is a column vector,

$$\boldsymbol{\delta\mu}_n|_i = \mu_i - \hat{\mu}_n(z_i) \tag{8}$$

is the vector of residuals, and $\mathbf{C}_{\rm SN}$ is the covariance matrix of the Pantheon data. In case of uncorrelated data ($C_{ij} = \delta_{ij}\sigma_i^2$)), we recover the formula used in Shafieloo (2007) and L'Huillier & Shafieloo (2017).

The χ^2 of the reconstruction $\hat{\mu}_n(z)$ is then defined as

$$\chi^2_n = \boldsymbol{\delta\mu}_n^{\rm T}\cdot\mathbf{C}_{\rm SN}^{-1}\cdot\boldsymbol{\delta\mu}_n, \tag{9}$$

and in this work we only consider reconstructions with $\chi^2 < \chi^2_{\Lambda{\rm CDM\ best\text{-}fit}}$.

The result of the smoothing procedure is thus $H_0\hat{d_{\rm L}}_n(z) = 10^{(\hat{\mu}_n-5)/5}$. Under the assumption of a flat Universe, we can obtain $h_n(z) = 1/({\rm d}\mathcal{D}_n(z)/{\rm d}z)$. Therefore, we obtain a non-exhaustive sample of plausible expansion histories, directly reconstructed by supernova data, and with no model assumption, which all give a better χ^2 to the Pantheon data than the best-fit ΛCDM model. This enables us to explore regions of the physical space of the expansion history beyond the flexibility of the concordance model that can fit the data reasonably well.

2.2 BAO measurements of cosmic distances and expansion history

The radial mode of the BAO measures $H(z)r_{\rm d}$, while the transverse mode provides $d_{\rm A}(z)/r_{\rm d}$, where

$$r_{\rm d} = \frac{c}{\sqrt{3}}\int_0^{1/(1+z_{\rm drag})}\frac{{\rm d}a}{a^2H(a)\sqrt{1+\frac{3\Omega_{\rm b}}{4\Omega_{\rm r}}a}} \tag{10}$$

is the sound horizon at the drag epoch $z_{\rm drag}$. We combined the Baryon Oscillation Spectroscopic Survey (BOSS) DR12 consensus values (Alam et al. 2017) and the extended-BOSS (eBOSS) DR14Q measurements (Zhao et al. 2018). We note that both BOSS DR12 and eBOSS DR14Q provide $H(z)r_{\rm d}/r_{\rm d,fid}$ and $d_{\rm A}(z)r_{\rm d,fid}/r_{\rm d}$ with $r_{\rm d,fid} = 147.78\,$Mpc. We also include the Dark Energy Survey DR1 (DES DR1) measurement of $d_{\rm A}/r_{\rm d}$ at $z = 0.81$ (The Dark Energy Survey Collaboration et al. 2017). We use these BAO data along with our reconstructions of the expansion history from supernova data as two independent sets of observations to test some key aspects of the concordance model.

2.3 Testing Λ Dark Energy

The solid black lines in Fig. 1 show the different reconstructed $\mathcal{D}(z)$, $h(z) = 1/\mathcal{D}'(z)$ and $Om(z)$ from Pantheon supernovae compilation where $Om(z)$ is defined as (Sahni et al. 2008):

$$Om(z) = \frac{h^2-1}{(1+z)^3-1} \tag{11}$$

We also show in Fig. 1 the BAO data points for these quantities. Since the BAO measure $H(z)r_{\rm d}$ and $d_{\rm A}(z)/r_{\rm d}$, to have a good sense of comparison within the context of the concordance model, we normalize them by $H_0r_{\rm d}$ from Planck 2015 (TTTEEE+LowP+Lensing) best fit ΛCDM model, and show on the top panel $\mathcal{D}(z) = (1+z)H_0r_{\rm d}d_{\rm A}(z)/(cr_{\rm d})$, in the middle panel $h(z) = H(z)r_{\rm d}/H_0r_{\rm d}$ and the corresponding

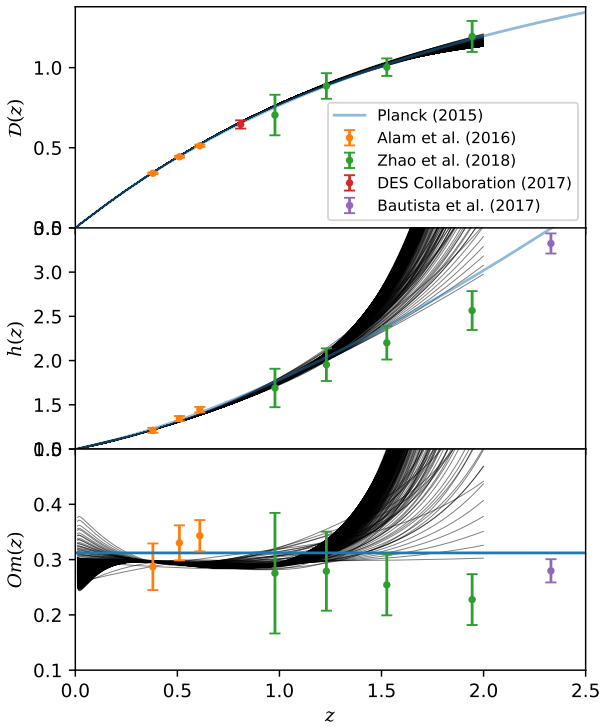

Figure 1. BAO data points normalized by $H_0 r_\mathrm{d}$ from (Planck Collaboration XIII 2016) best fit ΛCDM model. The black, solid lines are the reconstructed expansion histories from the Pantheon data which are fully model independent, and the purple line is the prediction from (Planck Collaboration XIII 2016) for the best-fit concordance ΛCDM model.

$Om(z)$ on the bottom panel. The magenta solid line shows the corresponding $\mathcal{D}(z)$, $h(z)$ and $Om(z)$ for the best-fit Planck 2015 Flat-ΛCDM model.

While the reconstructed expansion history $h(z)$ from SNIa are fully consistent with the BAO data points at low redshifts ($z \leq 1.2$), some tension seems to arise at higher redshifts ($z \geq 1.5$) where the reconstructed expansion histories from the BAO data suggest lower $h(z)$ with respect to the best fit ΛCDM model from Planck. While the errorbars are still quite large, the BAO data seem to follow the same trend in suggesting lower values of $h(z)$ (with respect to the best fit ΛCDM model from Planck) at high redshifts. For illustration purpose we also show the measurement of $h(z = 2.33)$ from the Lyman-α forest (Bautista et al. 2017) which seems to agree with other BAO data points suggesting lower $h(z)$ with respect to Planck best fit ΛCDM model, although we did not include this data point in our analysis since the supernovae data do not reach such a high redshift. This data point is consistent with the previous result from SDSS III (Delubac et al. 2015). This tension is also visible clearly looking at the Om diagnostic in bottom plot of Fig. 1, which is also consistent with the finding of (Sahni et al. 2014). If dark energy is a cosmological constant, the Om diagnostic should be constant in redshift. Therefore, having different values from different observations suggests some tension among the data within the framework of the concordance model.

Meanwhile, the comoving distances $\mathcal{D}(z)$ from BAO and SNIa are fully consistent together and with the best-fit Planck cosmology. Combining these results of the comoving distances and expansion histories may show some inconsistency with flatness as we will see later in this work.

2.4 Estimating $H_0 r_\mathrm{d}$

L'Huillier & Shafieloo (2017) estimated $H_0 r_\mathrm{d}$ in a model-independent way by combining BAO measurements and reconstructions of the expansion history from supernovae. For each reconstruction n, we can calculate $H_0 r_\mathrm{d}$ in two different ways

$$H_0 r_\mathrm{d}|_{d_\mathrm{A},n} = \frac{c}{1+z}\mathcal{D}_n(z)\frac{r_\mathrm{d}}{d_\mathrm{A}(z)} \tag{12a}$$

$$H_0 r_\mathrm{d}|_{H,n} = \frac{H(z) r d}{h_n(z)}, \tag{12b}$$

and their associated errors

$$\sigma_{H_0 r_\mathrm{d}}|_{d_\mathrm{A},n} = \frac{c}{1+z}\mathcal{D}(z)\frac{\sigma_{d_\mathrm{A}/r_\mathrm{d}}(z)}{(d_\mathrm{A}(z)/r_\mathrm{d})^2} \tag{13a}$$

$$\sigma_{H_0 r_\mathrm{d}}|_{H,n} = \frac{\sigma_{H r_\mathrm{d}}(z)}{h(z)}, \tag{13b}$$

where, assuming a flat-FLRW universe, $h(z) = 1/\mathcal{D}'(z)$.

Fig. 2 shows our estimation of $H_0 r_\mathrm{d}$ at the different BAO data points for the two estimations. In green is shown the Planck Collaboration XIII (2016) ΛCDM value. We can then define two error-bars. The first one is the error due to the supernova. At fixed redshift, we define $\langle H_0 r_\mathrm{d}\rangle_X$ as the median over all reconstructions for method $X \in \{d_\mathrm{A}, H\}$. We can then define the upper and lower limit as the minimal and maximal values of $H_0 r_\mathrm{d}|_{X,n}$. This error-bar is shown as a dashed line in Fig. 2. The second error is due to the uncertainty on the BAO (equations (13a) and (13b)), and is the uncertainty of the central value for a given reconstruction n. For each reconstruction n and method X, we have an error $\sigma_{H_0 r_\mathrm{d},X,n}$. They are of the same order for each reconstruction, so we define the final BAO error as the maximum value over all reconstructions. This error-bar is shown as a solid error-bar in Fig. 2.

For the first method (in orange), the measurements of $H_0 r_\mathrm{d}$ from combination of supernova and SDSS BAO data are fully consistent with Planck. The DES data point, also using the transverse BAO mode, is an independent confirmation at intermediate redshift. However, for the second method, while at low redshift, the measurements are consistent with Planck, the eBOSS data points are systematically lower than the Planck best-fit at $z \geq 1.2$ while the errorbars become very large at this range. This can be understood by the following remarks.

The first method yields very consistent results thanks to the use of the transverse BAO mode, which has smaller error-bars, coupled with direct reconstructions $\mathcal{D}(z)$ which do not use derivative.

The second method however, uses the line-of-sight mode of the BAO, together with $h(z)$ from supernovae data which is a derivative. Since the Pantheon data become scarce at $z \geq 1$, the estimation of $h(z)$ becomes less precise at this range having large error-bars. Combination of these two results to large uncertainties for $H_0 r_\mathrm{d}$ from the second method. On the other hand, it can be seen from Fig. 1 that while $h(z)$ from SNIa are higher than the best-fit Planck ΛCDM model, $h(z)$ from the BAO (scaled with best fit Planck ΛCDM

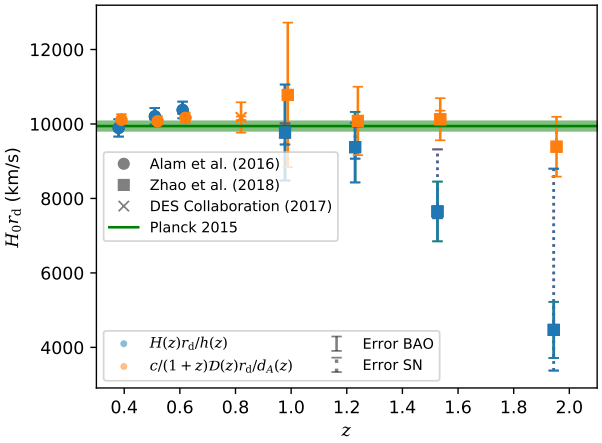

Figure 2. Model-independent measurement of $H_0 r_d$ estimated at the different BAO data points. The dotted error-bars show the range of possible central values from different reconstructions (SN error), while the solid error bars show the uncertainty on the central value (BAO error).

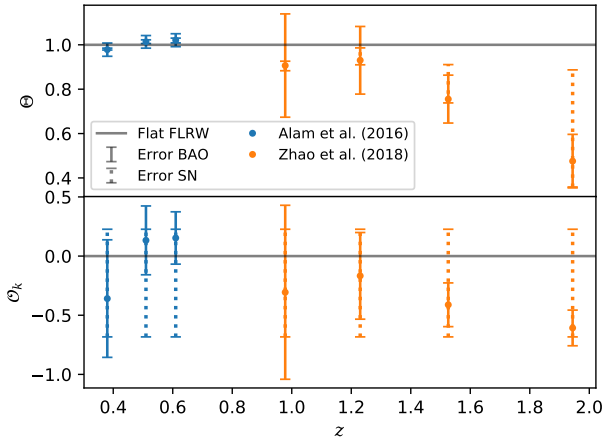

Figure 3. FLRW and curvature test: $\Theta(z)$ (top) and $O_k(z)$ (bottom). The dotted error-bars show the range of possible central values from different reconstructions (SN error), while the solid error bars show the uncertainty on the central value (BAO error). For a flat-FLRW Universe, $\Theta(z) \equiv 1$ and $O_k(z) \equiv \Omega_k$.

Table 1. Weighted average of $H_0 r_d$ from the H and d_A methods.

Method	$H_0 r_d$	Error SN	Error BAO
$\langle H_0 r_d \rangle_{d_A}$ (km s^{-1})	10120.42	$^{+33.79}_{-59.12}$	±103.92
$\langle H_0 r_d \rangle_{H}$ (km s^{-1})	9162.80	$^{+875.06}_{-921.02}$	±166.39

model) are actually lower. This explains the lower values of $H(z)r_d/h(z)$ at the eBOSS redshifts with respect to the other measurements.

We can then estimate, for each reconstruction n and method $X \in \{d_A, H\}$, the weighted average

$$\langle H_0 r_d \rangle_{X,n} = \sigma^{-2}_{H_0 r_d, X, n}\, \mathbb{1}^T \cdot C_n^{-1} \cdot \boldsymbol{H_0 r_d}|_{X,n}, \tag{14}$$

where

$$\sigma^2_{H_0 r_d, X, n} = \mathbb{1}^T \cdot C_n^{-1} \cdot \mathbb{1} \tag{15}$$

is the variance of the weighted average, and $\boldsymbol{H_0 r_d}|_{X,n}$ is a vector constituted of estimations of $H_0 r_d$ at different redshifts for iteration n. We report our results in Table 1. The Planck 2015 value of $H_0 r_d$ for the ΛCDM model is $(9944.0 \pm 127.4)\,\mathrm{km\,s^{-1}\,Mpc^{-1}}$. We should note an important interpretation of this result. While all our reconstructions of the expansion history from supernovae data have better χ^2 with respect to the best fit ΛCDM model, our large uncertainties on $H_0 r_d$ indicates that tight constrains on this quantity from model dependent approaches (such as assuming ΛCDM model) have limitations in expressing the reality of the universe and estimating its key parameters.

2.5 Test of the FLRW metric and the curvature

L'Huillier & Shafieloo (2017) reformulated the Clarkson et al. (2008) O_k diagnostic by introducing the Θ diagnostic so that it now only depends on the BAO and supernovae observables:

$$O_k(z) = \frac{\Theta^2(z) - 1}{\mathcal{D}^2(z)} \tag{16a}$$

$$\Theta(z) = h(z)\mathcal{D}'(z) = \frac{1+z}{c} H(z) r_d \frac{d_A(z)}{r_d} \frac{\mathcal{D}'(z)}{\mathcal{D}(z)}. \tag{16b}$$

For a FLRW Universe, $O_k(z) \equiv \Omega_k$, and in case of flatness, $O_k(z) \equiv 0$ and $\Theta(z) \equiv 1$. We can then calculate for each reconstruction n the associated $O_{k,n}(z)$ and $\Theta_n(z)$. Similarly to § 2.4, we calculated the median of O_k and Θ over all reconstructions, and defined the SN error as the minimal and maximal values, and the BAO error as the maximal error over all reconstructions. Fig. 3 shows $\Theta(z)$ (top) and $O_k(z)$ (bottom). Both are consistent with a flat FLRW metric up to $z \simeq 1.2$.

However, at high redshift, some deviation from flatness can be seen. Again, this can be explained by the previous remarks. In addition to the scarcity of the SN data at $z \geq 1.5$, which results in into poor constraints on $h(z)$, the BAO seem to show some internal tensions. While $d_A(z)/r_d$ are consistent with the Planck best-fit, $H(z)r_d$ are lower than expected. However, the Θ and O_k statistics assume a FLRW metric, where d_A and H are related to each other. Thus, discrepancy between d_A and H combined with the higher h values at high-redshift ($z \geq 1$) yields lower values for Θ and O_k.

3 GROWTH OF STRUCTURE VERSUS EXPANSION: TESTING GR

At the perturbation level, the cosmological growth of structure can also serve as a test of gravity (Nesseris & Perivolaropoulos 2008; Song & Percival 2009; Basilakos 2012; Shafieloo et al. 2013; Pavlov et al. 2014; Gómez-Valent et al. 2015; Ruiz & Huterer 2015; Mueller et al. 2016; Nesseris et al. 2017; Marra & Sapone 2017; Solà et al. 2017; Kazantzidis & Perivolaropoulos 2018). In the linear regime,

the growth of structure follows

$$\ddot{\delta} + 2H\dot{\delta} - 4\pi G\bar{\rho}\delta = 0, \tag{17}$$

where $\delta = \rho/\bar{\rho} - 1$ is the density contrast with respect to the mean density of the Universe $\bar{\rho}$. The growth rate

$$f(a) = \frac{\mathrm{d}\ln\delta}{\mathrm{d}\ln a} \tag{18}$$

can be approximated for a wide range of cosmologies by (Lahav et al. 1991; Wang & Steinhardt 1998; Linder 2005)

$$f(z) = \Omega_{\rm m}^{\gamma}(z), \tag{19}$$

where

$$\Omega_{\rm m}(z) = \frac{\Omega_{\rm m}(1+z)^3}{h^2(z)}. \tag{20}$$

In general relativity (GR), $\gamma \simeq 0.55$. $f\sigma_8$ is thus a powerful probe of gravity. Observationally, redshift-space distortion enables to measure the combination (e.g. Song & Percival 2009)

$$f\sigma_8(z) \simeq \sigma_8\Omega_{\rm m}^{\gamma}(z)\exp\left(-\int_0^z \Omega_{\rm m}^{\gamma}(x)\frac{\mathrm{d}x}{1+x}\right), \tag{21}$$

where $\sigma_8 = \sigma_8(z=0)$ is the rms fluctuation in $8\,h^{-1}$Mpc spheres. Following this formalism, having model independent reconstructions of the expansion history and $f\sigma_8(z)$ data, one can obtain constraints on $\Omega_{\rm m}$,γ, and σ_8 (L'Huillier et al. 2018).

Note, however, that one should keep in mind that Eq. (19) is an approximate fit only. In particular, γ may not be exactly constant for quintessence (dark energy modelled by a scalar field with some potential minimally coupled to gravity, Polarski et al. 2016). Still both for ΛCDM and for quintessence-CDM this fit is good since $\frac{\mathrm{d}\gamma}{\mathrm{d}z}$ is small as far as $\Omega_{\rm m}$ is not too small (see also Polarski & Gannouji 2008). For modified gravity theories like $f(R)$ gravity, the situation can be different (Gannouji et al. 2009; Motohashi et al. 2010).

3.1 Cosmological constraints on $\Omega_{\rm m}, \gamma, \sigma_8$

Following L'Huillier et al. (2018), we combined the Pantheon compilation with the latest measurements of $f\sigma_8$: 2dFGRS (Song & Percival 2009), WiggleZ (Blake et al. 2011), 6dFGRS (Beutler et al. 2012), VIPERS (de la Torre & Peacock 2013), the SDSS Main galaxy sample (Howlett et al. 2015), 2MTF (Howlett et al. 2017), BOSS DR12 (Gil-Marín et al. 2017), FastSound (Okumura et al. 2016), and eBOSS DR14Q (Zhao et al. 2018). In this section, we assume a flat Universe, therefore

$$h(z) = \frac{1}{\mathcal{D}'(z)}. \tag{22}$$

For each reconstructed expansion history $h_n(z)$, we vary $(\Omega_{\rm m}, \gamma, \sigma_8)$ and calculate $\widehat{f\sigma_8}(z|\Omega_{\rm m}, \gamma, \sigma_8, h_n)$ via eq. (21). We can then fit the RSD data and since the RSD and SN data are independent, we then calculate the total χ^2 by summing

$$\chi^2_{n,\rm tot} = \chi^2_{n,f\sigma_8} + \chi^2_{n,\rm SN}, \tag{23}$$

where

$$\chi^2_{n,f\sigma_8} = \boldsymbol{\delta f\sigma_{8n}} \cdot \mathbf{C}^{-1}_{f\sigma_8} \cdot \boldsymbol{\delta f\sigma_{8n}}, \tag{24}$$

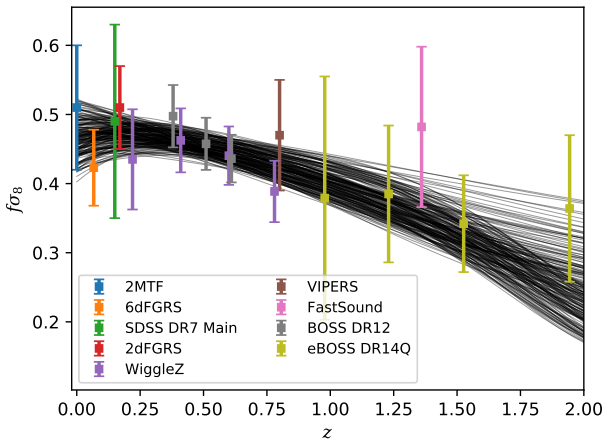

Figure 4. $f\sigma_8$ data used in this work from different surveys. The black lines are computed from eq. (21) using a random combination of expansion histories, $\Omega_{\rm m}$, γ, and σ_8. All lines have a better χ^2 to the SN+growth data than the best-fit ΛCDM model.

and where the ith component of the residual vector $\boldsymbol{\delta f\sigma_{8n}}$ is

$$\delta f\sigma_{8n}|_i = \widehat{f\sigma_8}_n(z_i|\Omega_{\rm m}, \gamma, \sigma_8, h_n) - f\sigma_8|_i. \tag{25}$$

The $f\sigma_8$ data used in this work are shown in Fig. 4. The black lines are computed from equation (21) using a randomly selected combination of expansion histories from supernovae data, $\Omega_{\rm m}$, γ, and σ_8. All lines have a better χ^2 to the SN+growth data than the best-fit ΛCDM model.

The red contours in the $(\sigma_8, \Omega_{\rm m})$ plane in Fig. 5a show the 1σ and 2σ regions of the parameter space in the flat ΛCDM case, that is, flat-ΛCDM expansion history and $\gamma = 0.55$. The blue contours in Fig. 5a show the allowed parameter space in the model-independent case. Namely, for any point in the blue contours, one can find at least one reconstruction $h(z)$ which, combined to the corresponding $(\Omega_{\rm m}, \gamma, \sigma_8))$, gives a better fit to the data than the best-fit ΛCDM. In the $(\sigma_8, \Omega_{\rm m})$ plane, the model-independent case is fully consistent with the ΛCDM case. Moreover, the flexibility of the model-independent approach allows a larger area of the parameter space to be consistent to the data. For instance, for larger values of σ_8 and lower values of $\Omega_{\rm m}$, one can find reconstructed expansion histories that give a better total fit to the data (SNIa+growth) with respect to the best fit ΛCDM model. For the model-independent case, γ is fully consistent with 0.55, as expected from GR. Moreover, lower value of γ, combined with lower value of $\Omega_{\rm m}$ and larger σ_8, can also provide good fit to the data.

We then fix $\gamma = 0.55$, as we did for the ΛCDM case, and show in Fig. 5b the corresponding confidence contours. This effectively allows for a non-ΛCDM background expansion, with gravity as GR. This time, since we do not allow γ to vary, the region with low $\Omega_{\rm m}$ and high σ_8 is now forbidden.

Finally, following L'Huillier et al. (2018), we focus on combinations of $h(z)$ and $\Omega_{\rm m}$ that respect the positive dark energy condition

$$\Omega_{\rm de}(z) = h^2(z) - \Omega_{\rm m}(1+z)^3 \geq 0 \qquad \forall z. \tag{26}$$

We show this region in dark-blue in Figs. 5a and 5b. Imposing equation (26) effectively forbids large values of

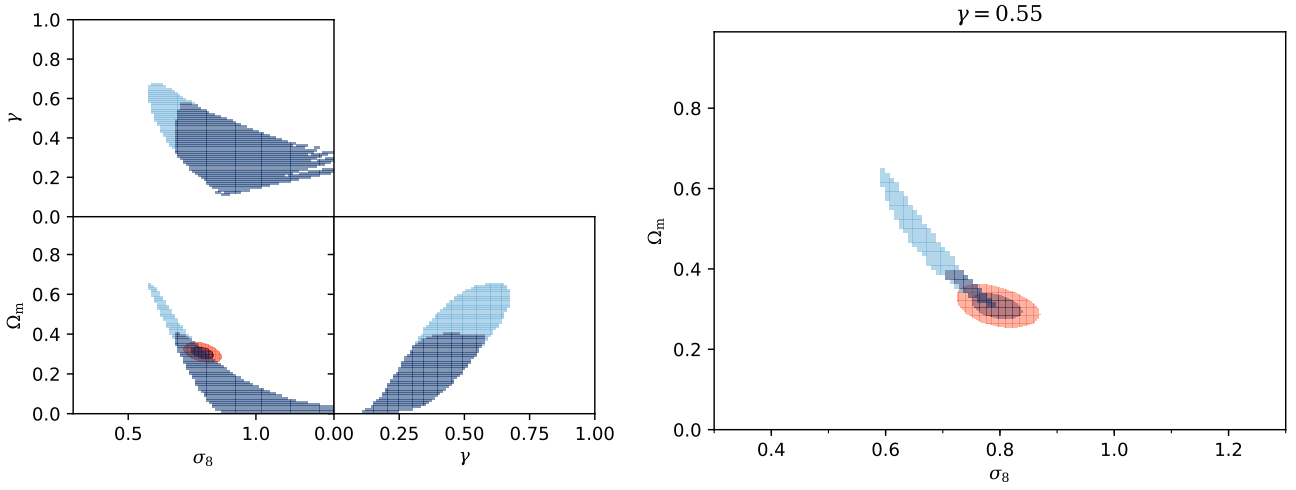

(a) (b)

Figure 5. Model independent cosmological constrains on $(\Omega_m, \gamma, \sigma_8)$ from growth and expansion data. In plot (b) we have fixed $\gamma = 0.55$ (assuming GR). The red contours are the 1σ and 2σ confidence levels for the ΛCDM case. The blue contours are associated to the combination of the parameters and reconstructions of the expansion history that yield a better χ^2 with respect to the best-fit ΛCDM model. The dark-blue region satisfy positive dark energy density condition as expressed in equation (26).

Ω_m, and dramatically reduces the allowed parameter space of the model-independent case. The allowed region of the parameter space is then fully consistent with the model-dependent case, as in L'Huillier et al. (2018). This is a strong support from the data for combination of ΛCDM and GR. Comparing our results here using most recent supernovae (Pantheon compilation) and BAO data (from eBOSS DR14) with what was reported in L'Huillier et al. (2018) we can notice substantial improvement on the constrains on these three key cosmological parameters. Based on our analysis we can now put strong model-independent upper bound limits on $\Omega_m < 0.42$ and $\gamma < 0.58$ and a lower bound limit on $\sigma_8 > 0.70$. These are in fact model independent constrains on these key cosmological parameters.

4 SUMMARY AND CONCLUSIONS

We used the Pantheon supernovae compilation to reconstruct the expansion history in a model-independent way, using an improved version of the iterative smoothing method (Shafieloo et al. 2006; Shafieloo 2007; L'Huillier & Shafieloo 2017), which we modified to take into account the non-diagonal terms of the full covariance matrix. We then combined the reconstructed expansion histories to measurements of $H(z)r_d$ and $d_A(z)/r_d$ from BOSS DR12 and eBOSS DR14Q to model-independently measure $H_0 r_d$ and test the FLRW metric. Our measurements of $H_0 r_d$ are consistent with the Planck 2015 values, while the metric test is consistent with a Flat-FLRW metric. However, for the eBOSS DR14Q data points, while $d_A(z)/r_d$ is consistent with the prediction from the Planck best-fit ΛCDM cosmology, the $H(z)r_d$ measurements are slightly but systematically lower. This yields some hints for a departure from flat-FLRW (Fig. 3) and supports previous findings of Sahni et al. (2014) & Zhao et al. (2017).

We then fit the growth data from redshift space distortion, mainly from SDSS survey using the model-independent reconstructions of the expansion history, and put model-independent constraints on $\Omega_m < 0.42$, $\gamma < 0.58$ and $\sigma_8 > 0.70$. Our measurements are fully consistent with the ΛCDM model with GR ($\gamma \approx 0.55$), and do not reveal any tension between the two data sets.

Future surveys, such as the Dark Energy Spectroscopic Instrument (DESI Collaboration et al. 2016a,b), the Large Synoptic Telescope (Ivezic et al. 2008), and WFIRST, will improve the quality and quantity of data, enabling us to detect any possible deviation from ΛCDM.

ACKNOWLEDGEMENTS

We thank Gongbo Zhao and Yuting Wang for stimulating discussions, and Dan Scolnic for providing the Pantheon data. The computations were performed by using the high performance computing clusters Polaris and Seondeok at the Korea Astronomy and Space Science Institute. A.S. would like to acknowledge the support of the National Research Foundation of Korea (NRF-2016R1C1B2016478). A.A.S. was partly supported by the program 0033-2018-0008 "Relativistic astrophysics and cosmology" from the FASO of the Russian Federation.

REFERENCES

Alam S., et al., 2017, MNRAS, 470, 2617
Basilakos S., 2012, International Journal of Modern Physics D, 21, 1250064
Bautista J. E., et al., 2017, A&A, 603, A12
Beutler F., et al., 2012, MNRAS, 423, 3430
Blake C., et al., 2011, MNRAS, 415, 2876
Clarkson C., Bassett B., Lu T. H.-C., 2008, Physical Review Letters, 101, 011301
DESI Collaboration et al., 2016a, preprint, (arXiv:1611.00036)

DESI Collaboration et al., 2016b, preprint, (arXiv:1611.00037)
Delubac T., et al., 2015, A&A, 574, A59
Denissenya M., Linder E. V., Shafieloo A., 2018, J. Cosmology Astropart. Phys., 3, 041
Farooq O., Ratra B., 2013, Physics Letters B, 723, 1
Gannouji R., Moraes B., Polarski D., 2009, J. Cosmology Astropart. Phys., 2, 034
Gil-Marín H., Percival W. J., Verde L., Brownstein J. R., Chuang C.-H., Kitaura F.-S., Rodríguez-Torres S. A., Olmstead M. D., 2017, MNRAS, 465, 1757
Gómez-Valent A., Solà J., Basilakos S., 2015, J. Cosmology Astropart. Phys., 1, 004
Howlett C., Ross A. J., Samushia L., Percival W. J., Manera M., 2015, MNRAS, 449, 848
Howlett C., et al., 2017, MNRAS, 471, 3135
Ivezic Z., et al., 2008, preprint, (arXiv:0805.2366)
Kazantzidis L., Perivolaropoulos L., 2018, preprint, (arXiv:1803.01337)
L'Huillier B., Shafieloo A., 2017, J. Cosmology Astropart. Phys., 1, 015
L'Huillier B., Shafieloo A., Kim H., 2018, MNRAS, 476, 3263
Lahav O., Lilje P. B., Primack J. R., Rees M. J., 1991, MNRAS, 251, 128
Linder E. V., 2005, Phys. Rev. D, 72, 043529
Marra V., Sapone D., 2017, preprint, (arXiv:1712.09676)
Motohashi H., Starobinsky A. A., Yokoyama J., 2010, Progress of Theoretical Physics, 123, 887
Mueller E.-M., Percival W., Linder E., Alam S., Zhao G.-B., Sánchez A. G., Beutler F., 2016, preprint, (arXiv:1612.00812)
Nesseris S., Perivolaropoulos L., 2008, Phys. Rev. D, 77, 023504
Nesseris S., Pantazis G., Perivolaropoulos L., 2017, Phys. Rev. D, 96, 023542
Okumura T., et al., 2016, PASJ, 68, 38
Pavlov A., Farooq O., Ratra B., 2014, Phys. Rev. D, 90, 023006
Planck Collaboration XIII 2016, A&A, 594, A13
Polarski D., Gannouji R., 2008, Physics Letters B, 660, 439
Polarski D., Starobinsky A. A., Giacomini H., 2016, J. Cosmology Astropart. Phys., 12, 037
Räsänen S., Bolejko K., Finoguenov A., 2015, Physical Review Letters, 115, 101301
Ruiz E. J., Huterer D., 2015, Phys. Rev. D, 91, 063009
Sahni V., Shafieloo A., Starobinsky A. A., 2008, Phys. Rev. D, 78, 103502
Sahni V., Shafieloo A., Starobinsky A. A., 2014, ApJ, 793, L40
Sapone D., Majerotto E., Nesseris S., 2014, Phys. Rev. D, 90, 023012
Scolnic D. M., et al., 2017, preprint, (arXiv:1710.00845)
Shafieloo A., 2007, MNRAS, 380, 1573
Shafieloo A., Alam U., Sahni V., Starobinsky A. A., 2006, MNRAS, 366, 1081
Shafieloo A., Kim A. G., Linder E. V., 2013, Phys. Rev. D, 87, 023520
Solà J., Gómez-Valent A., de Cruz Pérez J., 2017, Modern Physics Letters A, 32, 1750054
Song Y.-S., Percival W. J., 2009, J. Cosmology Astropart. Phys., 10, 004
The Dark Energy Survey Collaboration et al., 2017, preprint, (arXiv:1712.06209)
Wang L., Steinhardt P. J., 1998, ApJ, 508, 483
Zhao G.-B., et al., 2017, Nature Astronomy, 1, 627
Zhao G.-B., et al., 2018, preprint, (arXiv:1801.03043)
de la Torre S., Peacock J. A., 2013, MNRAS, 435, 743

This paper has been typeset from a TEX/LATEX file prepared by the author.